

Hydrogen-induced defects in niobium

J. Cizek^{a,*}, I. Prochazka^a, S. Danis^a, M. Cieslar^a, G. Brauer^b,
W. Anwand^b, R. Kirchheim^c, A. Pundt^c

^a Faculty of Mathematics and Physics, Charles University in Prague, V Holešovičkách 2, CZ-180 00 Praha 8, Czech Republic

^b Institut für Ionenstrahlphysik und Materialforschung, Forschungszentrum Rossendorf, Postfach 510119, D-01314 Dresden, Germany

^c Institut für Materialphysik, Universität Göttingen, Friedrich-Hund-Platz 1, D-37077 Göttingen, Germany

Received 12 September 2006; received in revised form 11 November 2006; accepted 13 November 2006

Available online 28 December 2006

Abstract

The introduction of new defects due to H-loading of Nb, their population as a function of the H concentration, and the mechanism of their formation are investigated by positron annihilation spectroscopy (PAS). In addition, X-ray diffraction (XRD), and transmission electron microscopy (TEM) are applied. Furthermore, the results obtained by the experimental techniques are compared with theoretical calculations of energetic stability and positron characteristics of various defect-H configurations. It is found that vacancies surrounded by H atoms are introduced into the specimens by H-loading. The density of these vacancy-H complexes increases with increasing concentration of H in the specimens. The H-induced vacancies are formed even in the α -phase field, when the metal-H system is a single phase solid solution. The stability of the H-induced defects and the mechanism of their formation are discussed.

© 2006 Elsevier B.V. All rights reserved.

Keywords: Metal hydrides; Point defects; Positron spectroscopies; X-ray diffraction

1. Introduction

It is known that H strongly interacts with open volume defects in a host metal lattice [1]. For example, H trapping at Cu vacancies was demonstrated already 28 years ago by positron annihilation spectroscopy (PAS) [2]. More recently, it was shown that H is not only trapped at existing defects, but a high amount of new defects can also be created by H-loading [3,4]. Nevertheless, the nature of the H-induced defects and the mechanism of their creation are still not completely understood.

One can notice that the behavior of H in metals is similar in some respects to that of a positron. Both H and positron exhibit a high mobility even at room temperature and both are trapped at open volume defects (e.g. vacancies, grain boundaries, etc.). Nowadays, PAS is a well-established tool in studying the properties of open volume defects in metals [5]. Positrons are emitted in the β^+ decay, e.g. by ^{22}Na radioisotope. Once a positron penetrates into a solid, it lowers very quickly its kinetic energy down to the thermal energy $\approx kT$. This process which takes

only a few picosecond is called thermalization. The thermalized positron diffuses in the solid and eventually becomes annihilated by one of the surrounding electrons. The electron-positron pair is converted predominantly into two anti-collinear γ -rays in the process of annihilation. The positron annihilation rate (i.e. the inverse of the positron lifetime) is given by an overlap of the positron and the electron wave functions. A free positron is delocalized in the lattice in a Bloch like state with the de Broglie wavelength around 5 nm at room temperature. An open volume defect represents a potential well for free positrons. As a consequence, a transition from the free positron state into the trapped state localized in the open volume defect is possible. The average electron density in an open volume defect is lower than in the bulk. The lifetime of trapped positrons is, therefore, increased compared to the value observed in a perfect lattice. The local electron density and, thereby, also the lifetime of trapped positrons differs in various kinds of defects. It enables to identify various defect types from their lifetimes observed in positron lifetime spectra.

Moreover, the detailed electronic structure information about a positron trapping site can be extracted from the measurement of the Doppler broadening of the annihilation radiation [5]. From the Doppler measurement, one obtains the one-dimensional

* Corresponding author. Tel.: +420 221912788; fax: +420 221912567.
E-mail address: jcizek@mbox.troja.mff.cuni.cz (J. Cizek).

momentum distribution of the annihilating electron–positron pairs. The low-momentum part arises mainly from annihilations with the valence electrons. On the other hand, the high-momentum part is mainly due to the core electrons which are tightly bound to the nuclei with specific binding energies and wave functions. Thus, the high-momentum part is characteristic for the local chemical environment where the annihilation event took place. The coincidence Doppler broadening (CDB) measurement of the two γ -rays emitted in the annihilation event leads to a significant reduction of background which enables a detailed analysis of the high-momentum parts (HMP's) of the spectra [6].

A high sensitivity to open volume defects, sensitivity to the local electronic structure of defects and the local chemical surrounding make PAS an ideal technique for investigations of H interaction with defects. In the present work, we employed a high-resolution positron lifetime (PL) spectroscopy combined with CDB. The positron annihilation studies of H interaction with defects in Nb were accompanied by X-ray diffraction (XRD) and transmission electron microscopy (TEM).

2. Experimental

Disk shaped (diameter ≈ 10 mm, thickness ≈ 0.5 mm) bulk Nb (99.9%) samples were firstly annealed (1000 °C/1 h) in vacuum. The aim of the annealing was to remove most of defects introduced into the sample during its previous history. Some samples were subsequently irradiated with 10 MeV electrons up to a fluence of $2 \times 10^{21} \text{ m}^{-2}$ ($T_{\text{irr}} \leq 100$ °C). The mean penetration depth of 10 MeV electrons into Nb is ≈ 2 mm, i.e. four times higher than the sample thickness. As a consequence the concentration of the irradiation-induced defects is nearly uniform in the whole sample volume. It was confirmed by PL measurements performed on the irradiated side of the sample and also on the opposite side. Both measurements gave nearly the same results. The surface of all samples was covered with a 30 nm thick Pd cup in order to prevent oxidation and to facilitate H absorption. The samples were step-by-step loaded with H by electrochemical charging [1]. We used a mixture of H_3PO_4 (85%) and glycerin (85%) in the ratio 1:1 as electrolyte. A low current density of $3.8 \times 10^{-3} \text{ mA mm}^{-2}$ was used in order to prevent hydrogen losses. Moreover, oxygen was removed from the electrolyte by slow bubbling with Ar and the H-loading was performed in a protective Ar atmosphere. The H concentration, x_{H} , in the sample was determined using the Faraday's law and is given by the atomic ratio H atoms/Nb atoms in the whole paper. The relative accuracy of determination of x_{H} was estimated to be 5%. The defect studies were performed by PL spectroscopy using a fast-fast PL spectrometer with timing resolution of 160 ps [7], CDB studies were carried out using a spectrometer described in Ref. [8]. A ^{22}Na positron source with activity

of 1.5 MBq was used. The mean penetration depth of positrons emitted by ^{22}Na into Nb is $\approx 30 \mu\text{m}$. The calculations of the positron lifetimes were performed by the atomic superposition method (ATSUP) [9] using 128 Nb atom supercells, see [10] for details. The HMP curves were calculated using a method described in Ref. [11]. The lattice expansion was measured by XRD on Philips Expert diffractometer using Cu $K\alpha$ radiation. TEM observations were performed on the JEOL 2000 FX electron microscope operating at 200 kV.

3. Results and discussion

3.1. Annealed Nb

The annealed Nb can be considered as a “defect-free” material because it exhibits a single component PL spectrum with a lifetime $\tau_{\text{B}} = 128$ ps, which agrees well with the calculated bulk Nb lifetime [10]. The dependence of the positron lifetimes on the H concentration x_{H} is plotted in Fig. 1a. When the sample was H-loaded in the α -phase range ($x_{\text{H}} < 0.06$), a new component with a lifetime $\tau_2 \approx 150$ ps appeared in the PL spectra. It is a contribution of positrons trapped at new defects created by H-loading. The intensity I_2 of this component is plotted in Fig. 1b. One can see in Fig. 1 that the lifetime τ_2 remains approximately constant, while I_2 strongly increases with x_{H} . It shows that the nature of the H-induced defects does not change and their concentration increases with increasing H content in the sample. The H-induced volume expansion in the α -phase field is an elastic, reversible process. Thus, we do not expect the formation of dislocations, which are often introduced by precipitation of hydrides. Indeed, no additional dislocations were observed in the H-loaded samples by TEM. Based on Refs. [3,4], vacancies are considered to be the most probable candidates for the H-induced defects. The lifetime τ_2 is, however, remarkably shorter than that of positrons trapped at Nb mono-vacancies characterized by $\tau_{\text{v}} = 222$ ps [10]. A natural explanation of such a short lifetime is that the H-induced vacancies are surrounded by H atoms.

Theoretical calculations performed in Ref. [10] revealed that a H atom trapped at a vacancy in Nb is not situated directly in the center of the vacancy, but located on a line between the vacancy center and the nearest neighbor octahedral interstitial position at a distance of about 0.12 nm away from the vacancy center. There are six such positions (crystallographically equivalent) around one vacancy. A H atom situated in the vicinity

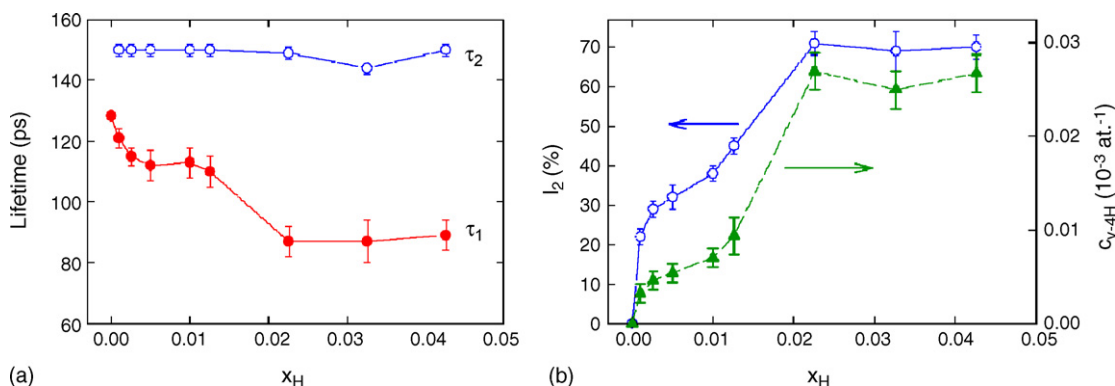


Fig. 1. (a) The lifetimes of the exponential components resolved in PL spectra of the annealed Nb sample as a function of H concentration x_{H} ; (b) the relative intensity I_2 of trapped positrons (open circles) and the concentration of the H-induced vacancies (full triangles) as a function of x_{H} .

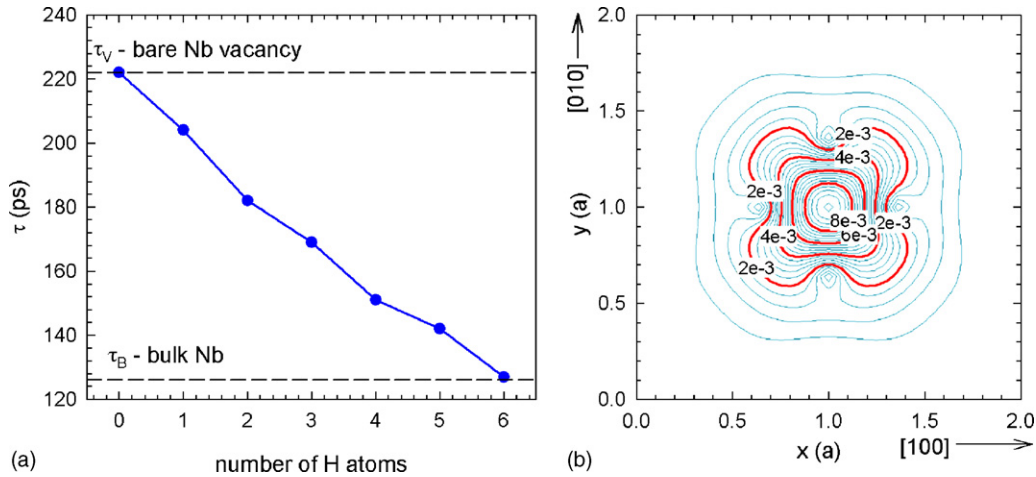


Fig. 2. (a) The calculated lifetime of positrons trapped in the H-induced vacancy as a function of the number of H atoms surrounding the vacancy; (b) the calculated positron density in the (001) plane for the vacancy surrounded by four H atoms. The x- and y-axis are scaled in the relative units related to the lattice constant a . The vacancy is situated at the 110 coordinates.

of a vacancy causes an increase of the local electron density and, thereby, a decrease of the lifetime of trapped positrons. Fig. 2a shows the calculated lifetime of trapped positrons as a function of the number of H atoms surrounding the vacancy. Obviously, an increasing number of H atoms surrounding the vacancy causes a monotonic decrease of the lifetime of trapped positrons from $\tau_v = 222$ ps for a H-free vacancy down to 127 ps for a vacancy surrounded by 6 H atoms (v-6H), i.e. all the six positions filled with H. The lifetime of about 150 ps observed in the experiment corresponds to a vacancy surrounded by 4 H atoms (v-4H). Thus, we conclude that v-4H complexes are introduced by H-loading in Nb in the α -phase field. The calculated positron density for a v-4H is shown in Fig. 2b.

The concentration of the H-induced vacancies was calculated from the two-state trapping model [12] using the trapping coef-

ficient $\nu = 1 \times 10^{14}$ atoms/s and is plotted in Fig. 1b. One can see in the figure that the concentration of v-4H defects is approximately three orders of magnitude lower than x_H . Thus, most of H occupies the regular tetrahedral interstitial positions (T_H) in the Nb lattice, while only a small fraction of H formed vacancies and is trapped in the vicinity of them. However, the number of H-induced vacancies is similar to that created by a thermal heat treatment close to the melting point.

In the present work, we performed a “loading–unloading” experiment with the purpose to test the stability of the H-induced vacancies. The annealed sample was firstly step-by-step H loaded, i.e. the H-induced vacancies were created. The dependence of the intensity I_2 of positrons trapped at v-4H complexes on x_H during the loading is plotted in Fig. 3a (upper panel). The concentration c_{v-4H} of the v-4H defects calculated from the

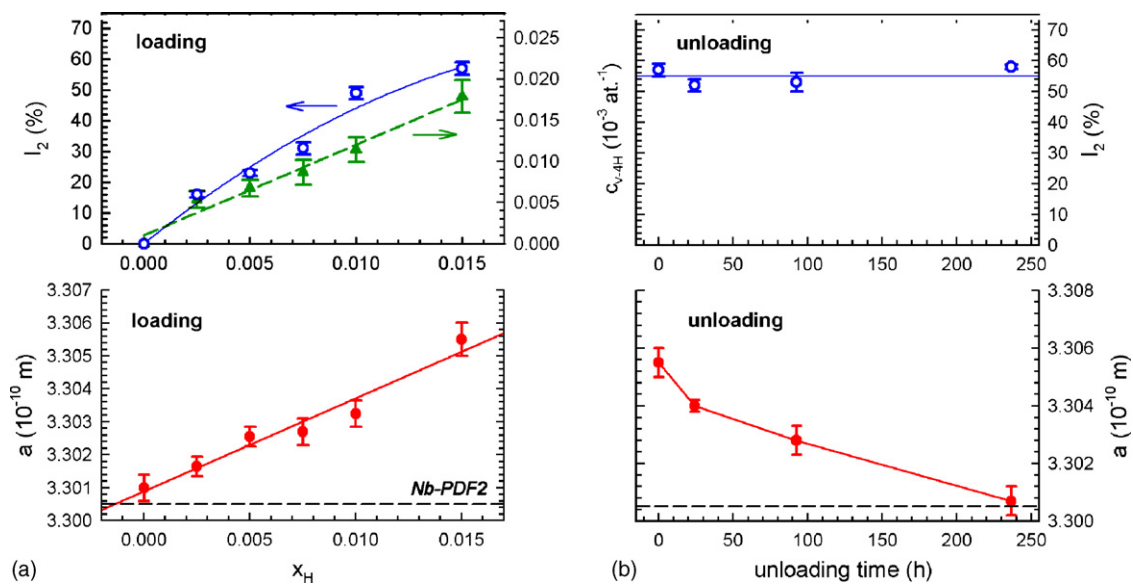


Fig. 3. The H “loading–unloading” experiment. (a) Loading—the intensity I_2 of trapped positrons (open circles), the concentration c_{v-4H} of H-induced v-4H complexes (full triangles), and the lattice constant a (full circles, lower panel) as a function of H concentration x_H . (b) Unloading—the intensity I_2 of trapped positrons (open circles), the lattice constant a (full circles, lower panel) as a function of the unloading time.

Table 1
Positron lifetimes τ_i and relative intensities I_i resolved in the PL spectra of irradiated Nb samples

Sample	τ_1 (ps)	I_1 (%)	τ_2 (ps)	I_2 (%)	τ_3 (ps)	I_3 (%)	c_{v-2H} (10^{-5} at. $^{-1}$)	c_{v-H} (10^{-5} at. $^{-1}$)
Nb bare irradiation	43(8)	14(2)	182 Fix	61(2)	204 Fix	25(3)	10.7(5)	4.9(5)
Nb bare irradiation + Pd cap after irradiation	44(9)	14(2)	182 Fix	57(2)	204 Fix	29(4)	10.2(5)	5.3(5)
Nb irradiation with Pd cap	48(5)	15(2)	182 Fix	74(1)	204 Fix	11(3)	12.0(7)	1.8(5)

The lifetime τ_2 and τ_3 were fixed at 182 ps (v-2H) and 204 ps (v-H), respectively. The concentration of v-2H and v-H complexes calculated from the three-state trapping model are shown in the last two columns. The errors given in parentheses correspond to the last digit.

two-state trapping model is plotted in Fig. 3a as well. The H-loading leads to a lattice expansion which is seen as an increase of the lattice constant a (Fig. 3a, lower panel). At $x_H = 0.015$ the loading was stopped and the sample was subsequently electrochemically unloaded using a constant voltage $U = 0.8$ V of opposite polarity. One can see in Fig. 3b that the lattice constant returned to that for the H-free Nb sample. This suggests that H in the interstitial T_H lattice positions was removed by unloading. On the other hand, I_2 and also the lifetime $\tau_2 = 150$ ps remain unchanged during unloading. It testifies that the vacancy-trapped H is not removed and the v-4H complexes are present also in the unloaded specimen.

3.2. Electron-irradiated Nb

Three samples are compared: irradiated bare Nb, the former sample with a Pd cap sputtered after irradiation, and Nb irradiated with Pd cap. A two-component fit of PL spectra resulted in a defect component with a lifetime in the range of 191–184 ps, i.e. remarkably shorter than $\tau_v = 222$ ps. This indicates that vacancies created by irradiation are associated with H. From a comparison with Fig. 2a, one can deduce that the irradiated samples contain a mixture of v-H and v-2H complexes. Hence, in the final analysis of the PL spectra, we fixed the known lifetimes 182 ps (v-2H) and 204 ps (v-H) and decomposed the spectra into three components. The results are shown in Table 1. Clearly, the dominant defects in the irradiated samples are of the type v-2H. Sputtering of the Pd cap after the irradiation does not change the defect structure. On the other hand, the sample irradiated with Pd cap exhibits a higher ratio of concentrations of v-2H to v-H complexes, i.e. it contains more H.

This is most probably due to the catalytic effect of Pd which facilitates dissociation of H_2 molecule on the surface [13]. We suggest that H trapped at vacancies in the irradiated samples comes from the air, namely from the water vapor molecules dissociated by the energetic electrons in the course of irradiation.

A H atom attached to a vacancy could be directly identified by CDB. To check this possibility we calculated HMP curves for a Nb vacancy surrounded by a various number of H atoms. The calculated HMP's are plotted in Fig. 4a as ratio curves related to the bulk Nb in order to magnify the differences at high momenta. Prior to the discussion of the profiles, it should be mentioned that the calculated HMP's do not contain the contribution from the valence electrons and a comparison with the experiment is, therefore, meaningful only for momenta higher than about $8 \times 10^{-3} m_0 c$, i.e. in the region shown by a hatched mark, see Fig. 4a, where the contribution of valence electrons becomes negligible. One can see in the figure that the presence of H attached to a vacancy leads to the appearance of a peak like feature (indicated by an arrow) centered at $15 \times 10^{-3} m_0 c$ in the ratio HMP curve. This contribution increases with increasing number of H atoms surrounding the vacancy. The experimental HMP ratio curves measured by CDB on the irradiated samples are plotted in Fig. 4b. One can see that the experimental curves exhibit a well-pronounced peak at $15 \times 10^{-3} m_0 c$, i.e. at the same position as in the theoretical HMP curves. Such a good qualitative agreement in shape of the experimental and the calculated HMP curves testifies that the irradiation-induced vacancies are surrounded by H. Moreover, this “hydrogen peak” is higher in the sample irradiated with Pd cap which is known to contain more H.

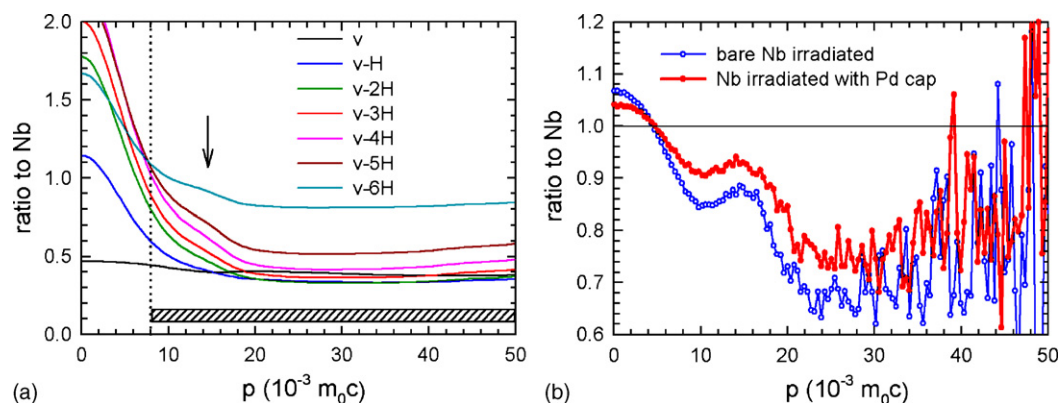


Fig. 4. (a) the calculated HMP ratio curves for a bare Nb vacancy (v) and a Nb vacancy surrounded by n H atoms (v- n H); (b) the experimental HMP ratio curves for the electron irradiated Nb.

4. Conclusions

New defects were created in annealed Nb by H-loading in the α -phase field. A comparison of the experimental data with theoretical calculations indicates that the H-induced defects are vacancies surrounded by four H atoms. The concentration of the H-induced defects is roughly three orders of magnitude lower than the H concentration in the sample and increases with increasing content of H in the sample. It was shown that the H-induced vacancy-H complexes are stable and cannot be removed by electrochemical unloading, while the H which occupies the regular tetrahedral interstitial sites was removed. It was found that vacancies introduced into Nb by electron irradiation are surrounded by H. The electron irradiated Nb samples contain most probably a mixture of v-2H and v-H complexes. Thus, vacancy-H complexes in annealed and electron irradiated samples are not identical. It has been demonstrated that H attached to a vacancy can be identified by CDB.

Acknowledgements

Financial support from the Czech Science Foundation (Project No. 202/05/0074), the Ministry of Education of The Czech Republic (Project No. MS 0021620834), the INTAS (Project INTAS-05-1000005-7672) and the Alexander von

Humboldt Foundation is highly acknowledged. The authors are grateful to J. Kuriplach for providing them with the ATSUP code.

References

- [1] R. Kirchheim, Prog. Mater. Sci. 32 (1988) 261–325.
- [2] B. Lengeler, S. Mantl, W. Triftshäuser, J. Phys. F 8 (1978) 1691–1698.
- [3] Y. Fukai, N. Okuma, Phys. Rev. Lett. 73 (1994) 1640–1643.
- [4] Y. Shirai, H. Araki, T. Mori, W. Nakamura, K. Sakaki, J. Alloys Compd. 330 (2002) 125–131.
- [5] P. Hautojärvi, A. Vehanen, Positrons in Solids, in: P. Hautojärvi (Ed.), Topics in Current Physics, vol. 12, Springer-Verlag, Berlin, 1979, pp. 1–22.
- [6] K.G. Lynn, J.E. Dickman, W.L. Brown, M.F. Robbins, E. Bonderup, Phys. Rev. B 20 (1979) 3566.
- [7] F. Becvar, J. Cizek, L. Lestak, I. Novotny, I. Prochazka, F. Sebesta, Nucl. Instrum. Methods A 443 (2000) 557–577.
- [8] J. Cizek, I. Prochazka, B. Smola, I. Stulikova, R. Kuzel, Z. Matej, V. Cherkaska, Phys. Status Solidi (a) 203 (2006) 466–477.
- [9] M.J. Puska, R.M. Nieminen, J. Phys. F, Metall. Phys. 13 (1983) 333–346.
- [10] J. Cizek, I. Prochazka, F. Becvar, R. Kuzel, M. Cieslar, G. Brauer, W. Anwand, R. Kirchheim, A. Pundt, Phys. Rev. B 69 (2004) 224106.
- [11] J. Kuriplach, A.L. Morales, C. Dauwe, D. Segers, M. Sob, Phys. Rev. B 58 (1998) 107475.
- [12] P. Hautojärvi, C. Corbel, in: A. Dupasquier, A.P. Mills (Eds.), Proceedings of the International School of Physics “Enrico Fermi”, Course CXXV, IOS Press, Varena, 1995, pp. 491–562.
- [13] Q.M. Yang, G. Schmitz, S. Fähler, H.U. Krebs, R. Kirchheim, Phys. Rev. B 54 (1996) 9131–9140.